UCRL-16856

University of California

Ernest O. Lawrence Radiation Laboratory

THE KINETICS OF THE DISSOLUTION AND DIFFUSION OF DIVALENT COBALT OXIDE IN SODIUM DISILICATE GLASS

TWO-WEEK LOAN COPY

This is a Library Circulating Copy which may be borrowed for two weeks. For a personal retention copy, call Tech. Info. Division, Ext. 5545

Berkeley, California

DISCLAIMER

This document was prepared as an account of work sponsored by the United States Government. While this document is believed to contain correct information, neither the United States Government nor any agency thereof, nor the Regents of the University of California, nor any of their employees, makes any warranty, express or implied, or assumes any legal responsibility for the accuracy, completeness, or usefulness of any information, apparatus, product, or process disclosed, or represents that its use would not infringe privately owned rights. Reference herein to any specific commercial product, process, or service by its trade name, trademark, manufacturer, or otherwise, does not necessarily constitute or imply its endorsement, recommendation, or favoring by the United States Government or any agency thereof, or the Regents of the University of California. The views and opinions of authors expressed herein do not necessarily state or reflect those of the United States Government or any agency thereof or the Regents of the University of California.

Special
Thesis

UCRL-16856

UNIVERSITY OF CALIFORNIA

Lawrence Radiation Laboratory
Berkeley, California

AEC Contract No. W-7405-eng-48

THE KINETICS OF THE DISSOLUTION AND DIFFUSION OF DIVALENT COBALT OXIDE IN SODIUM DISILICATE GLASS

Alton Monroe Lacy
(M. S. Thesis)

May 5, 1966

THE KINETICS OF THE DISSOLUTION AND DIFFUSION OF DIVALENT COBALT OXIDE IN SODIUM DISILICATE GLASS

Contents

Abstract v

I. Introduction 1

II. Diffusion Theory 2

III. Experimental 6

A. Diffusion Couple Preparation 6

1. Glass 6

2. Oxide Substrate 6

3. Construction of the Diffusion Cell 7

B. Diffusion Heatings 7

1. Furnace Construction 7

2. Melting, Sealing and Diffusion 11

3. Preparation for Microprobe Analysis 12

C. Electron Microprobe Analysis 12

1. Description of the Microprobe 12

2. Experimental Procedure for Analysis 13

IV. Results 15

V. Discussion 28

A. Location of the Matano Interface 28

B. Comparison of the Diffusion of FeO with CoO in NS_2 . . 31

C. Determination of the Position of the Original Interface Based on a Mass Balance of all Oxides 34

D. The Question of the Existence of Other Oxides of Cobalt in the System $xCoO\text{-}yNS_2$ 35

E. Comment 36

VI. Conclusions 37

VII. Acknowledgment 38

VIII. References 39

THE KINETICS OF THE DISSOLUTION AND DIFFUSION OF DIVALENT COBALT OXIDE IN SODIUM DISILICATE GLASS

Alton Monroe Lacy

Inorganic Materials Research Division, Lawrence Radiation Laboratory, and Department of Mineral Technology, College of Engineering, University of California, Berkeley, California

May 5, 1966

ABSTRACT

The dissolution and diffusion of CoO in sodium disilicate glass was studied over the temperature range 900-1050°C. Diffusion couples were prepared in an inert atmosphere and analyzed with the electron microprobe. The mathematics of binary diffusion were applied to the resulting diffusion profiles and diffusivities were calculated based on (1) a constant diffusivity independent of concentration, and (2) Boltzmann-Matano analysis. The temperature dependence of diffusivity based on the former analysis may be expressed as

$$D = 8.05 \times 10^{-2} \exp(-35.4 \text{ Kcal/RT})$$

Expressions based on Boltzmann-Matano analysis are given in the text of this study. It was found that the diffusivity of CoO was lower and activation energy higher than similar values for FeO as determined by Borom.[7] This is interpreted in the light of differences in ionic polarizability. A discussion of the location of the Matano interface and original glass-oxide interface is also given.

I. INTRODUCTION

A thorough knowledge of the dissolution and diffusion kinetics of metal oxides in glass matrices has not only a practical interest (for instance, in the fields of glass to metal seals and enameling), but also is of a valuable theoretical interest in developing an insight into the structure of glass and an awareness of those parameters which govern atomic motion through a glass system under the influence of an activity gradient.

This study has been undertaken as part of a project to investigate the behavior of several transition metal oxides when put in contact with a molten glass--the results of which will hopefully form a reasonably sound basis for understanding and predicting the mechanisms of diffusion of other oxides in other glassy structures.

II. DIFFUSION THEORY

According to Crank,[1] diffusion is a process by which matter is transported from one part of a system to another as a result of random molecular motions in an attempt to reach some equilibrium state. This process may involve the transfer of one material into another, resulting in an overall mass transfer; or may be characterized by a redistribution of atoms or other molecular species within a single phase. The latter is referred to as self-diffusion, in which no mass transfer is evident. Analysis of the motion of material either within a single phase or between multiple phases may be analyzed by a number of methods, the most prominent of which are chemical analyses of consecutive sections of the diffusion couple, radioactive tracer techniques and electron microprobe analysis.

The mathematical theory of diffusion was first established by Fick,[2] whose first and second laws lay the groundwork for practically all diffusion studies. Fick's first law may be written as

$$J_i = -D \frac{dc_i}{dx} \tag{1}$$

where J_i = the flux of species i passing a plane of unit area per unit time, c_i = the concentration of species i per unit volume of material, and D is a constant of proportionality which is called the diffusion coefficient or diffusivity. If, in the diffusion process, there is a mass transfer, D represents the inter-diffusivity of species i; if no mass transfer takes place, D is referred to as the self-diffusion coefficient. Fick's first law assumes a constant D, and a flux transfer dependent only on the concentration gradient present.

If, however, a steady state does not exist, and the concentration

at some point is changing with time, Eq. (1) (although still valid) is not a convenient form to use.

Fick's second law more readily describes most real situations by including a concentration-time gradient, and may be expressed as

$$\frac{dC}{dt} = \frac{\delta}{\delta x}\left(D\frac{\delta c}{\delta x}\right) + \frac{\delta}{\delta y}\left(D\frac{\delta c}{\delta y}\right) + \frac{\delta}{\delta z}\left(D\frac{\delta c}{\delta z}\right) \qquad (2)$$

If one assumes diffusion only in one dimension, Eq. (2) may be reduced to

$$\frac{dC}{dt} = \frac{\delta}{\delta x}\left(D\frac{\delta c}{\delta x}\right) \qquad (3)$$

The units of D are usually given as cm^2/sec.

A number of texts[1,3,4] are available which present solutions of the diffusion equations for specific initial and boundary conditions. For the condition of binary diffusion of species i from a constant source into a semi-infinite medium, Crank[1] has given the solution to (3) as

$$M_t = 2C_s\ (Dt/\pi)^{1/2} \qquad (4)$$

where M_t is the total amount of diffusing substance which has left the source after time t; C_s is the surface concentration of i; and D is the apparent diffusivity, which is assumed constant and independent of concentration. Rearranging into the form

$$(M_t/C_s)^2 = 4Dt/\pi \text{ or } y = mx, \qquad (5)$$

we can see that the diffusivity D could readily be determined from the slope of a plot of $(M_t/C_s)^2$ vs. t.

In real systems, diffusivity of a species is rarely constant over a broad concentration range and consequently, the above solution is not strictly valid for more than a very short interval. If one assumes a variable diffusivity, another solution to (3) must be found. The

appropriate solution was first proposed by Boltzmann[5] and its initial application in metallic systems was made by Matano.[6] Boltzmann's solution of (3) assuming concentration dependent diffusion from a constant source into a semi-infinite medium is given as

$$D(c) = \frac{1}{2t}\left(\frac{dx}{dc}\right)\int_{c=0}^{c=c} x\,dc \qquad (6)$$

if the following conditions hold:

(1) The position of the original interface is known, i.e., x_M is defined by $\int_0^{c=c_o} x dc = 0$, (6a)

and is generally referred to as the Matano interface. (See Fig. 8.)

(2) The process is diffusion controlled, i.e., $x_{c=c_1} = kt^{1/2}$ (6b)

(3) At t=0, $c_i=0$ for $x>0$

$c_i=c_o$ for $x<0$

D is generally found by plotting c vs x and from this, $\frac{dx}{dc}$ (the reciprocal slope) may be calculated; and $\int_0^c x\,dc$ (the shaded area under the curve - Fig. 1) may be found by graphical integration.

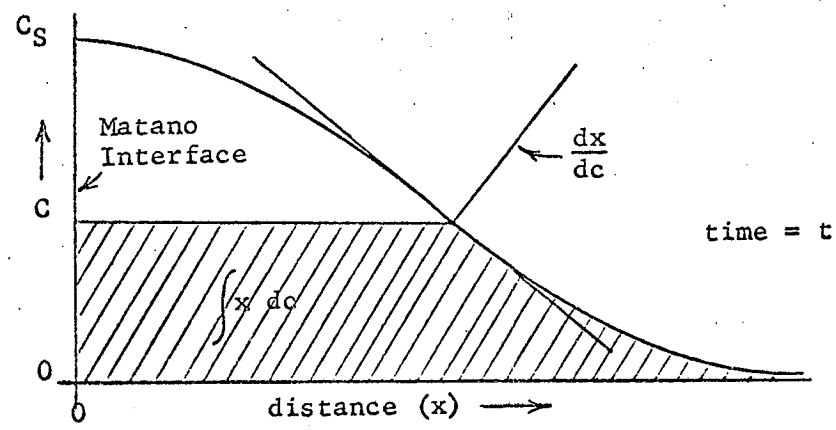

Fig. 1. Graphical representation of the quantities described by Eq. (6).

As well as being a function of concentration, the diffusivity is also a function of temperature. The nature of this temperature dependence is given by the equation

$$D = D_o \exp(-\Delta H/RT) \tag{7}$$

where D_o is a constant incorporating the mean free path of atomic movement, the lattice vibration frequency and the entropy of activation ($\exp(\Delta S/R)$). The enthalpy of activation (ΔH), (referred to as "activation energy") and the pre-exponential term (D_o) may be found by rearranging (7) to

$$\ln D = \ln D_o - \frac{\Delta H}{R}\left(\frac{1}{T}\right) \text{ or} \tag{8a}$$

$$\log_{10} D = \log_{10} D_o - \frac{\Delta H}{2.303R}\left(\frac{1}{T}\right) \tag{8b}$$

and subsequently plotting $\log_{10}$ (or ln) D vs (1/T). From the slope and intercept of the curve, these quantities may be determined.

III. EXPERIMENTAL

A. Diffusion Couple Preparation

1. Glass

Degassed sodium disilicate glass (NS_2) rod approximately 5/8 in. in diameter was prepared by Corning Glass Works in Corning, New York. This glass was smelted in vacuo in a Pt container at 1480° C and held at 0.015 torr for 2 hours before a cane was drawn in an argon atmosphere. The final composition of the glass as determined in the laboratories of Lawrence Radiation Laboratory was reported as 32.9% Na_2O-67.1% SiO_2. One-half inch lengths of the rod were cut to serve as diffusion specimens. The ends were then polished to an optical finish on SiC papers and diamond wheels. This was done to allow sighting through the specimen onto the oxide prior to melting, and also to reduce the surface entrapment of gases as much as possible to avoid bubbles at the interface upon vacuum sealing of the glass to the oxide. All rods were then cleaned in acetone and stored in a vacuum dessicator until ready to be used.

2. Oxide Substrate

Approximately 1/2 in. discs of 1/16-1/8 in. thick 99.5% Co metal were formed by grinding on a lap belt. The flat surfaces were polished on emery papers and diamond wheels to a smooth bright finish. A small hole was drilled in each disc, and a series of discs were hung by a Pt wire in the vertical furnace, (shown in Fig. 3). The arrangement was then lowered in vacuum into the hot zone of the furnace at 1000° C. Water-saturated air was introduced, and the Co metal was allowed to oxidize for approximately 4 hours. Subsequent examination showed a

smooth firmly attached oxide layer about 150 microns thick. X-ray examination showed only CoO. The oxidized discs were then stored in vaccuum to avoid formation of Co_3O_4 and Co_2O_3 on their surfaces.

3. Construction of the Diffusion Cell

The diffusion couple was formed by very carefully placing an oxidized CoO disc in the bottom of a Coors CN-5 recrystallized Al_2O_3 crucible. These crucibles are about 1 in. high and 5/8 in. in diameter. A cleaned and polished glass slug was then placed on top of the disc. The crucible and contents were placed in a graphite sample bucket fitted with a $Pt\text{-}Pt_{90}Rh_{10}$ thermocouple to monitor the sample temperature (see Fig. 2), and the arrangement was hung in the upper portion of the furnace.

B. Diffusion Heatings

1. Furnace Construction

The furnace used in this series of experiments was constructed by Borom;[7] a schematic diagram is shown in Fig. 3. It is a vertical resistance wound (Kanthal) furnace capable of operation to about 1200° C in either vacuum or controlled atmosphere. The power input is controlled by a series of external taps and rheostats which allow the operator to produce any desired thermal gradient. In this series of experiments, a gradient of less than ±1/2° C was maintained over the length of the diffusion sample. Typical power and thermal gradients are shown in Fig. 4. The sample bucket is attached to a vertical 4-hole porcelain rod which also contains the thermocouple leads. The rod extends up the length of the furnace and out through a Wilson seal. By this arrangement, the sample could be readily raised or lowered in

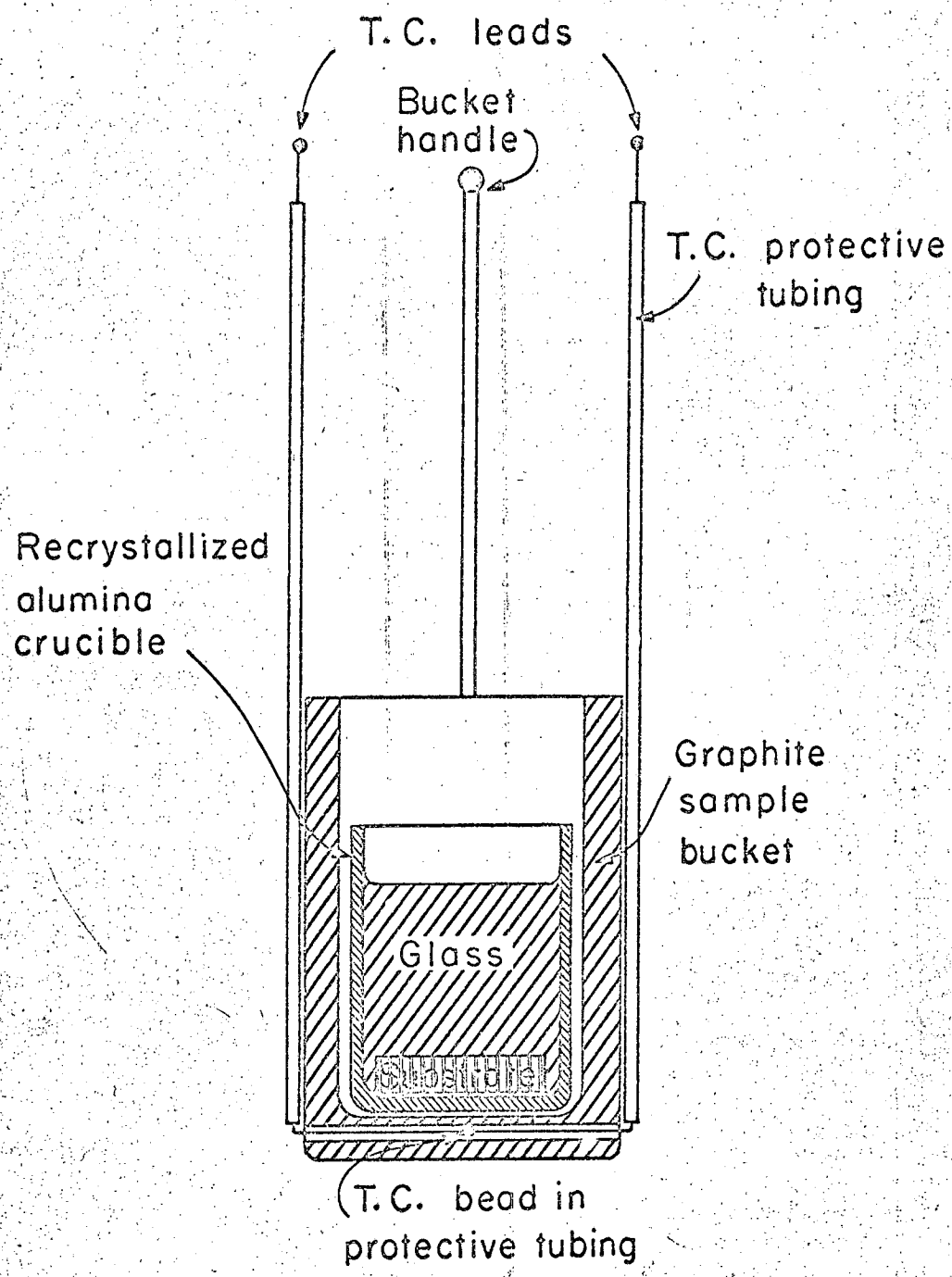

Fig. 2. Schematic diagram of the diffusion cell.

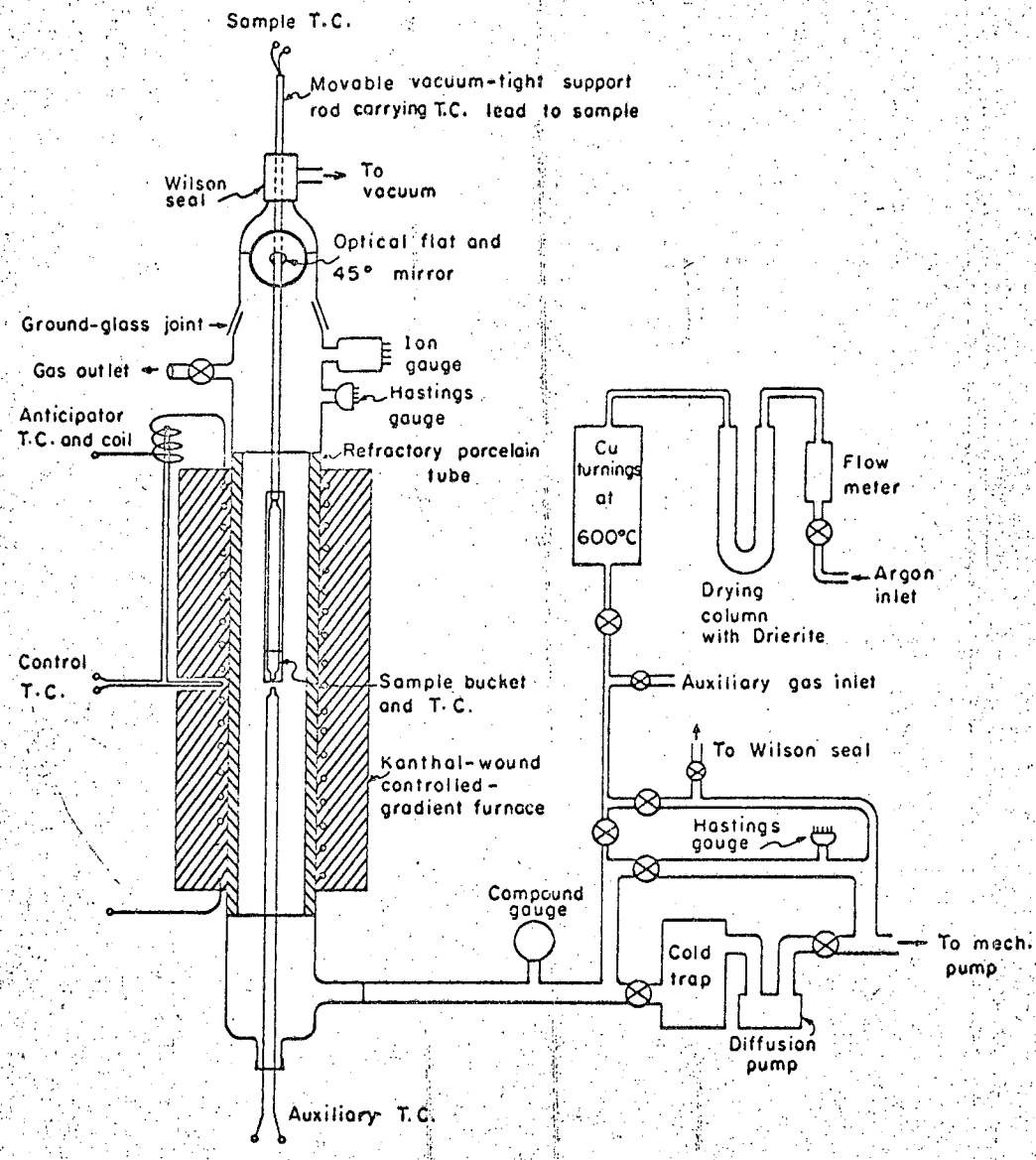

Fig. 3. Schematic diagram of diffusion furnace.

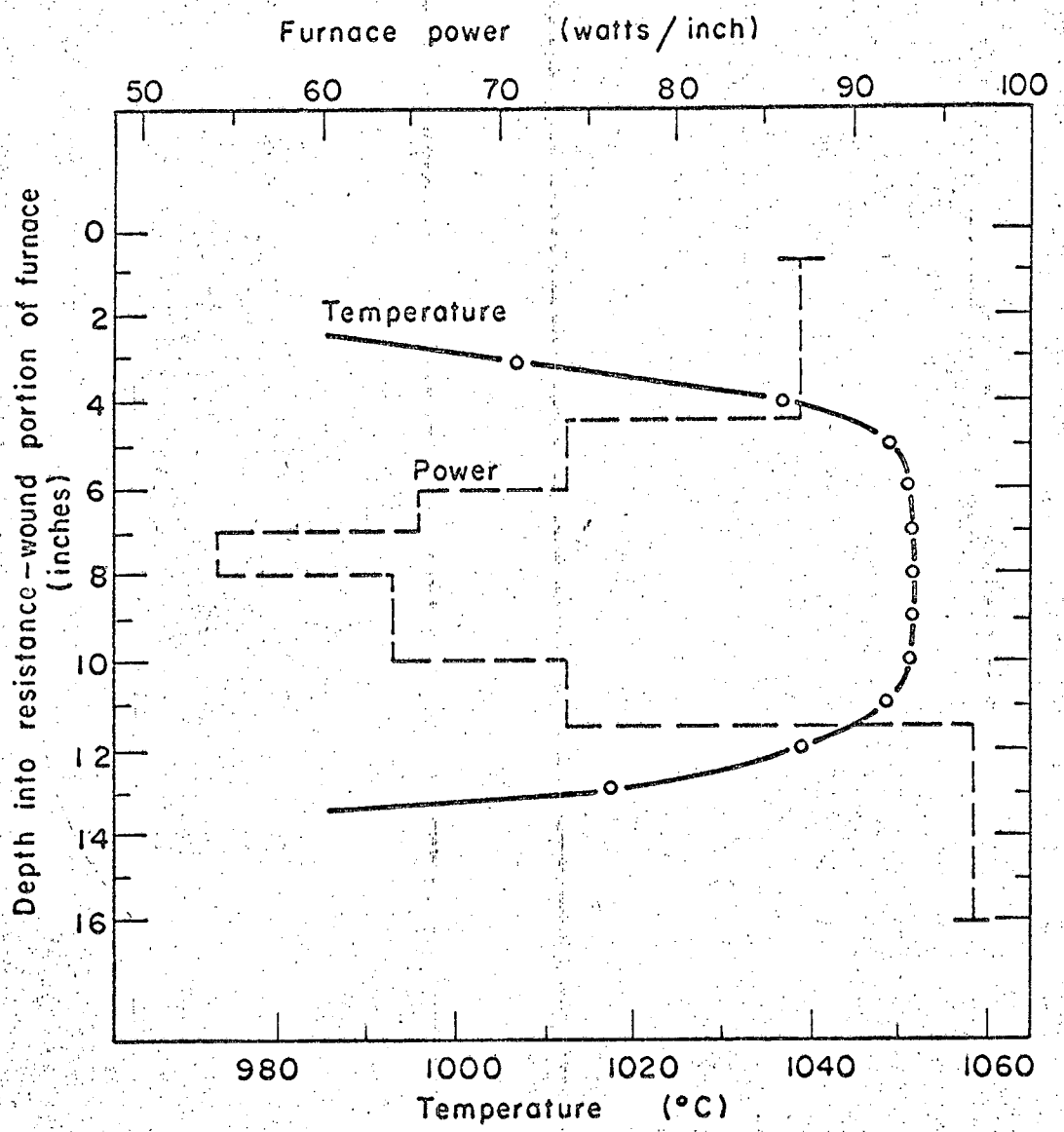

Fig. 4. Plot of typical furnace temperature and power gradients.

the furnace by manual manipulation, without a loss of vacuum of introduction of foreign gases. A mirror was situated at the upper end of the furnace to allow observations of the heating and melting process.

2. Melting, Sealing and Diffusion

Once the diffusion couple was placed in the graphite bucket, the entire assembly was hung on the end of the vertical porcelain rod, and this was set into position at the top of the furnace. The furnace was then evacuated to about 10^{-4} mm Hg, and the sample was lowered into a zone of the furnace where the temperature was about 550° C at the position of the oxide-glass couple. This temperature was below the softening point of the glass (598° C). The specimen remained in this position overnight to allow for maximum outgassing of the assembly. During this period, the pressure was maintained at 5×10^{-6} mm Hg. The sample temperature was recorded automatically on a Leeds and Northrup adjustable-span, adjustable range (ASAR) speedomax recorder. After outgassing, the sample was lowered into the "hot zone" of the furnace, and allowed to melt and seal around the oxidized cobalt disc. After melting had occurred, purified argon gas was introduced into the furnace and allowed to flow through at a very slow rate. The argon pressure was maintained at 1 atm. The purpose of the argon was (1) to reduce the loss of sodium by vaporization in vacuum, (2) to prevent the entry of atmospheric oxygen into the furnace, and (3) to reduce any convection which might occur from the evolution of entrapped gas within the sample or at the interface.

Once the sample had reached a temperature less than 50° C from the experimental temperature, the scale of the recorder was changed from

10 mv. to 2 mv. full scale, and adjusted to the range of the diffusion temperature. It was found that the test temperature was reached within 5-7 minutes after lowering, and the diffusion time was measured from approximately -5% of the test temperature. During the run, the temperature was controlled to an average ± 2° C.

At the end of the run, the sample was withdrawn rapidly to a zone where the temperature was around 550-600° C, and held there for at least 30 minutes to anneal. It was then slowly cooled to room temperature by gradual withdrawal and subsequently removed for sectioning.

3. Preparation for Microprobe Analysis

After removal from the furnace, the sample was mounted in clear plastic casting resin. A slice was taken through the center of the diffusion sample perpendicular to the oxide surface and parallel to the direction of diffusion. The section was then remounted in plastic so as to expose the diffusion surface. This was polished on SiC papers and diamond wheels (to 1/2-2 micron grit), resulting in an optical finish on the surface. Following this operation, it was vapor-coated with carbon to make the surface electrically conductive, and analyzed with the electron microprobe.

C. Electron Microprobe Analysis

1. Description of the Microprobe

Basically the electron microprobe is a device which impinges a finely focused electron beam onto a polished sample surface. Characteristic fluorescent x-rays are produced for each element in the sample. These are selectively diffracted by preset crystal spectrometers and their intensity measured with an appropriate counter. By calculation

or comparison with the intensities from standards of known composition, a quantitative analysis of the bombarded surface may be obtained. The probe is designed either to allow the investigator to focus the beam on a fixed specimen, or to translate the specimen under the beam, giving an integrated count over the length of traverse.

The electron microprobe used in this study was made by the Applied Research Laboratories and was capable of resolving separately the $K\alpha$ radiation of Si, Co, and Na. Each wave length is detected by a different counter and automatically printed out by an attached electric typewriter.

2. Experimental Procedures for Analysis

It was found that in electron microprobe investigation of these glasses that the bombardment of the sample by the electron beam results in a destruction of the surface and a subsequent change in the integrated count with time for a given fixed spot as sodium is vaporized under the beam. The result of this effect is to introduce serious error in any quantitative determinations which are to be made. To overcome this difficulty, the specimen was translated at a rate of 96 microns/min. in a direction parallel to the interface and normal to the direction of diffusion. This procedure continuously exposes fresh undamaged surface to the electron beam. The counts are integrated over a period of 20 sec. and then printed out.

In this study, integrated counts were taken at the interface and at 10, 20 or 50 micron intervals away from the interface until a constant composition (0% Co) was reached.

In order to afix quantitative values to the probe sample data, standard glasses of the composition (xNS_2-yCoO) were prepared. These

were subsequently quantitatively chemically analyzed by wet chemical means. Fragments of each composition were mounted together in plastic, polished and analyzed with the probe. A plot of probe counts vs. weight per cent CoO and SiO_2 resulted in a series of calibration curves from which the compositions of other glasses in the same series could be determined from their individual probe data.

The specific probe conditions used in this study were 15kV, 0.03 μ-amps sample current, beam dia.=~2μ, heavy carbon coating, scan parallel to the interface at 96μ/min. and integrate counts for 20 sec. for each scan. Although the Na peak could be resolved by the spectrometer, these conditions were found by Borom[7] to reduce the Na count data to only semi-quantitative value. However, due to an accuracy of ± 1-2% in the Co and Si analyses, the weight percent Na was determined by difference.

The use of standard glasses which are very similar in composition to the diffusion couple eliminates the necessity of corrections such as those due to absorption, secondary fluorescence, background radiation and other effects which would arise if one were calculating intensities based on theoretical considerations only. Since the count rate is not extremely high, no dead time corrections were necessary.

IV. RESULTS

The general experimental data for each diffusion run may be seen in Table II. Figure 5 shows the type of diffusion-concentration profile which results from electron microprobe analysis of this system. The example shown in this case is specimen 900-2 but the general shape of the curves are typical for all specimens.

In the analysis of diffusion data, the most simple and straightforward approach is to assume a constant diffusivity (at any given temperature), independent of concentration. This leads to the application of Crank's[1] solution to Fick's law (Eqs. (4) and (5)). It has been mentioned that the diffusivity (D) for any particular temperature may be readily evaluated from the slope of a plot of $(M_t)^2$ vs. time. Such a plot may be seen in Fig. 6. The temperature variation of diffusivity is given by Eqs. (7), (8a) and (8b). By applying the method of least squares to an Arhennius plot of (D) vs. (1/T), (Fig. 7), the activation energy (ΔH) and (D_o) are evaluated. The experimental data for this analysis may be seen in Table I, resulting in a value of $D_o = 8.05 \times 10^{-2}$ and an activation energy of -35.4 kcal. The diffusivity of CoO may then be written as a function of temperature as

$$D = (8.05 \times 10^{-2}) \exp(-35.4 \text{ kcal}/RT) \qquad (9)$$

Although the foregoing method gives reasonably linear plots, it does not completely exclude the possibility of a small concentration dependence of diffusivity, which is otherwise assumed to be within the range of experimental error. In order to ascertain whether this is the case, one may use the Boltzmann-Matano approach for diffusivity determination.

Table I. Experimental data for calculation of diffusivity independent of concentration.

Temp (°C)	w/o CoO C_s	$(4C_s^2)$	Slope (m)x10^5	π(m)x10^5	$D = \frac{\pi m_2}{4C_s}$ (cm/sec.2)	$\log_{10}D$	1/T(°K^{-1}) x 10^3
900	22.7	2061	0.8868	2.786	1.352x10^{-8}	0.13098-8	0.8525
950	23.2	2153	1.828	5.743	2.667x10^{-8}	0.42602-8	0.8177
1000	23.7	2247	2.986	9.817	4.369x10^{-8}	0.64038-8	0.7855
1050	24.1	2323	6.049	19.003	8.180x10^{-8}	0.91275-8	0.7559

According to Borom,[7] in order to apply the Boltzmann-Matano approach, it is first necessary to determine the position of the original glass-oxide interface prior to diffusion. If one assumes a constant density of the diffusing species, this position may be defined by the expression $\int_0^{c=c} x\,dc$ in a diffusion plot of c vs. x. This is illustrated by Fig. 8.

Table II. Experimental Conditions.

Sample Designation	Time (sec.)	Temperature (°C)	Interface Conc. (C_s)-w/o CoO	M_t w/o.cm.	CoO dissolved (microns)	Average* Density of $xCoO\text{-}yNS_2$ glass
900-1	3600	900±2		0.2012	8.6	2.76
900-2	7200	900±2	22.7	0.2475	10.7	2.79
900-4	14400	900±2		0.3574	15.6	2.81
950-1	3600	950±2		0.2956	12.7	2.76
950-2	7200	950±2	23.2	0.3571	15.4	2.78
950-4	14400	950±2		0.5130	22.2	2.79
1000-1	3600	1000±2		0.3474	14.9	2.76
1000-2	7200	1000±2	23.7	0.4734	20.5	2.79
1000-4	14400	1000±2		0.6382	27.3	2.81
1050-1	3600	1050±2		0.4673	20.3	2.80
1050-2	7200	1050±2	24.1	0.6600	28.8	2.82

* Density of glass at that distance from the interface dividing the area under the CoO diffusion profile in half.

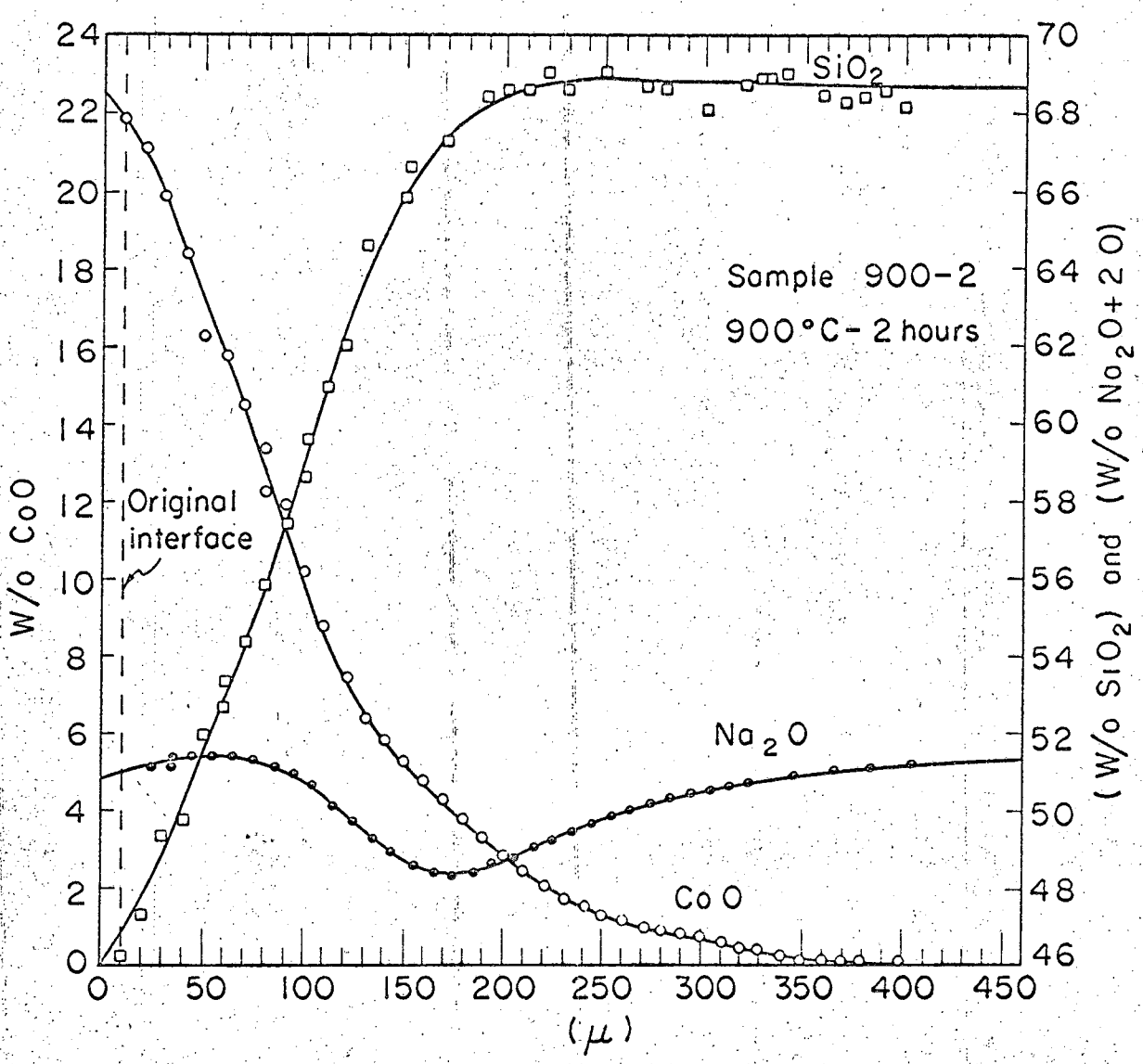

Fig. 5. 900-2 diffusion profiles for CoO, Na_2O and SiO_2

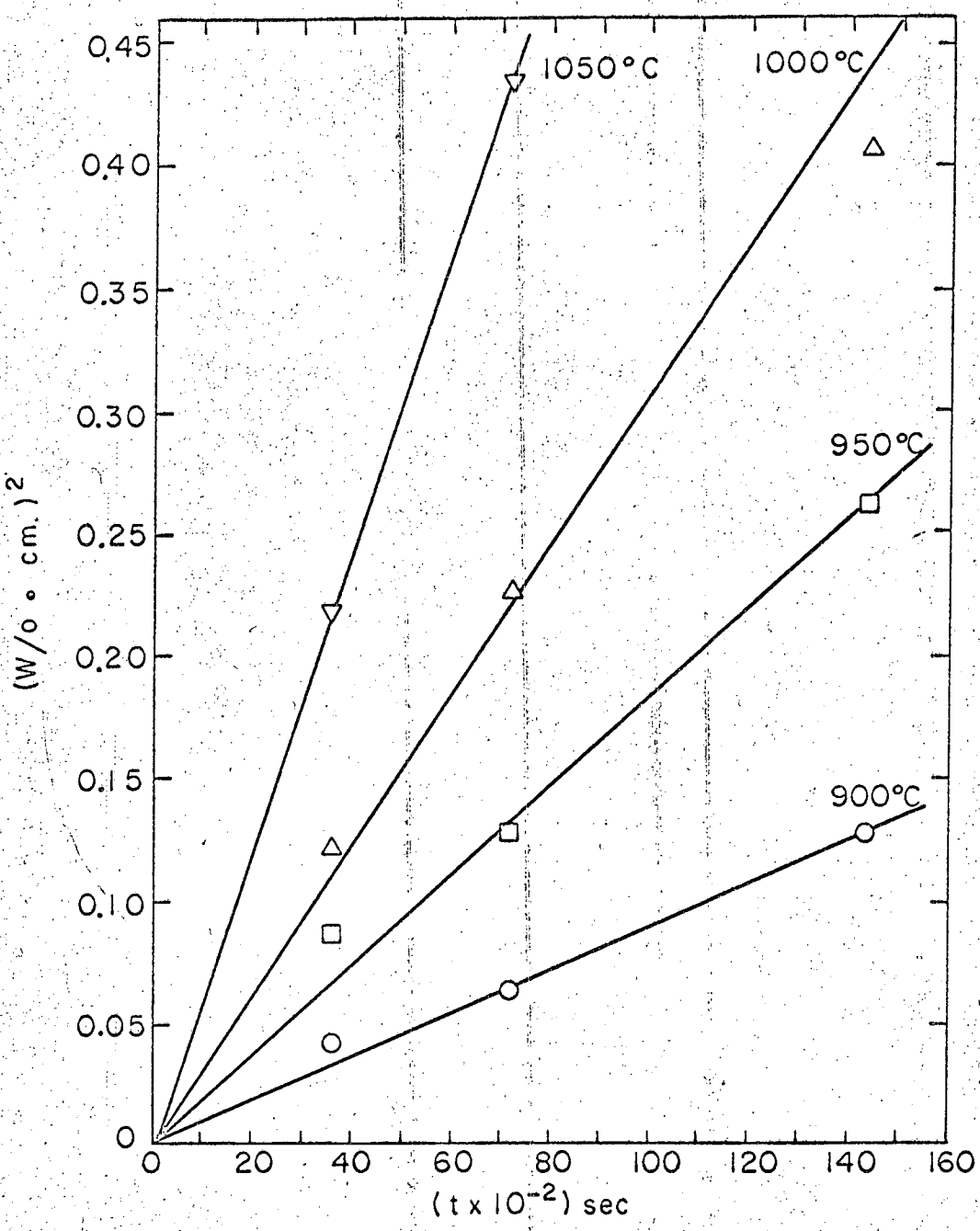

MUB-10891

Fig. 6. Plot for diffusivity determination according to Eq. (5).

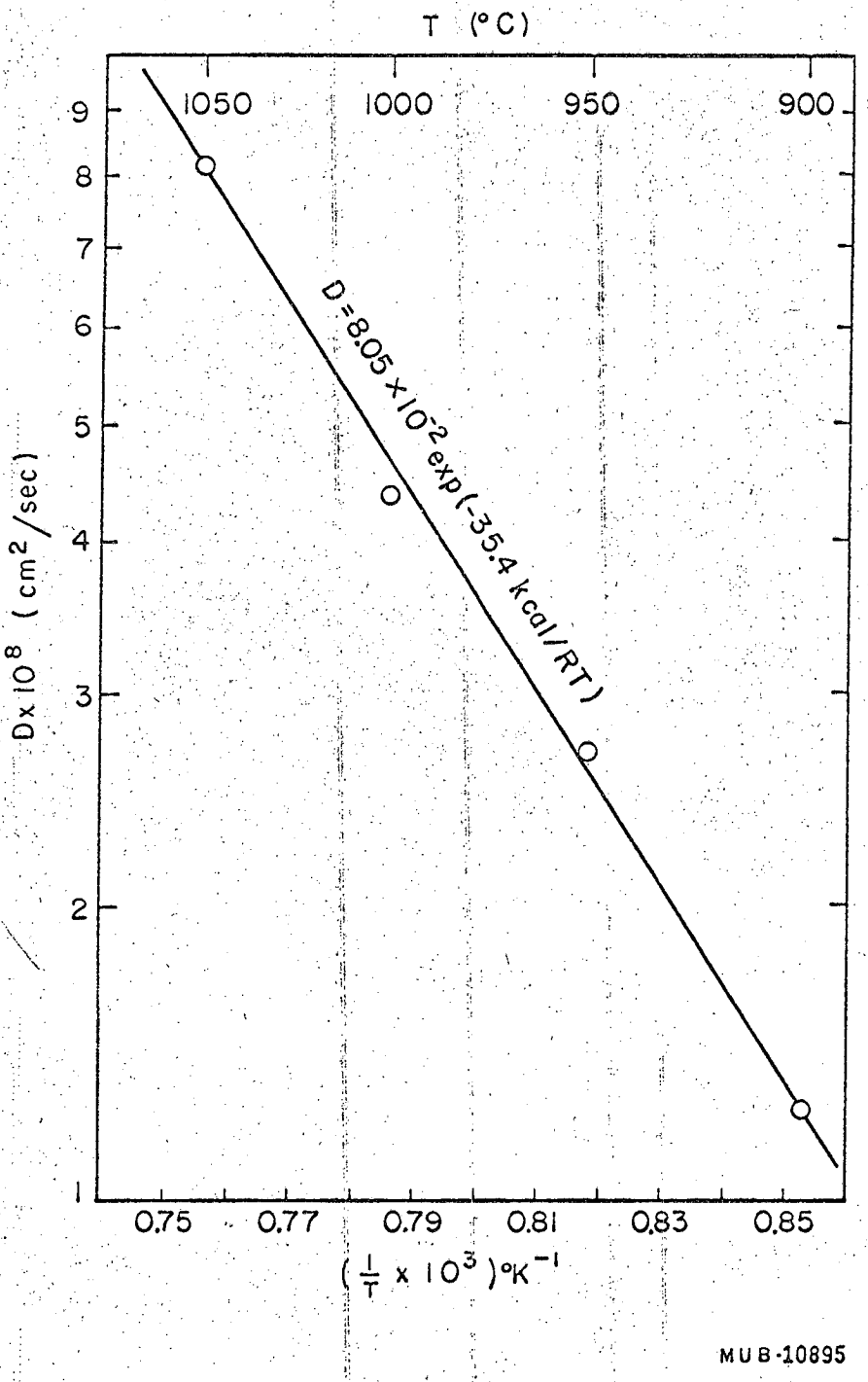

Fig. 7. Arhennius plot of the apparent diffusivities of CoO in NS_2 (as determined by the method of Eq. (5).

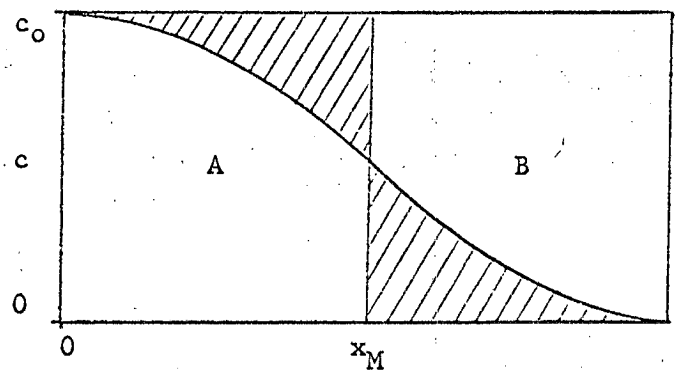

Fig. 8. Schematic diffusion profile for the diffusion of substance A into B indicating the position of the Matano interface according to Eq. (6a).

Since the shaded areas of Fig. 8 represent the amount of material which has left region A and moved into region B, a mass balance defines the original interface as the position where the areas are equal. For the case of a change in the density of the dissolving species (as in the dissolution of crystalline CoO in glass, with no glass penetration into the oxide layer), we cannot simply equate areas to determine the position of the original interface, but must include the densities of the CoO and $xCoO\text{-}yNS_2$ glass. This is necessary because the areas on the diffusion profile represent volumes of material, and in order to achieve a mass balance, each area must be multiplied by the density of its diffusion component. We may then locate the original interface using the expression:

$$(100 \text{ wgt\%. cm})\ (x)\ (\rho_{CoO}) = (A \text{ wgt\%. cm})_{glass} (\rho)_{glass} \qquad (10)$$

where (x) is the graphical position of the old interface relative to the new phase boundary; (ρ) is the density of the respective material; and (A) is the total area under the diffusion profile. Since the density of glass varies from the interface to the point of zero% CoO, it is

necessary to assume an average for the purpose of calculation. This is done by choosing the density of the glass composition at a distance from the interface which divides the area under the diffusion profile in half. In this study the "average" density ranged from 2.76-2.82. The density of CoO was taken as 6.45. The original interfaces calculated in this manner may be seen in Table II.

A computer program[8] was used to obtain the areas and reciprocal slopes (c.f. Fig. 1) from the diffusion profiles and to obtain solutions to Eq. (6). A typical plot of the computer determined diffusivity vs. mole fraction (n_{CoO}) is shown in Fig. 9. From these plots, D values were picked (for constant n = 0.03, 0.06, 0.09, 0.12 and 0.15) for each temperature; averaged, and plotted vs. (1/T). The results may be seen in Figs. 10 and 11. A least squares analysis of each Arhennius plot resulted in the temperature dependences of D as shown in Tables IIIa and IIIb.

It may be noted that, as the diffusion anneals are prepared, the diffusion temperature is not immediately reached. Consequently there must be a measure of judgment on the part of the experimenter regarding when to initiate timing the run (i.e. when t = o). The result of this is to increase the experimental "time" error inherent in the shorter diffusion runs. On this basis, it would therefore seem logical to put more confidence in the 4-hour data than the 2-hour data, with the least confidence in the 1-hour data. As a step toward minimizing this error, each value of D was "weighted" in accordance with the time of the diffusion anneal. If one then "weights" the 4-hour anneal by a factor of 4, the 2-hour anneal by a factor of 2, and the 1-hour anneal

by 1; and subsequently averages D for the three times, the temperature variation of diffusivity may be expressed as in Table IIIb.

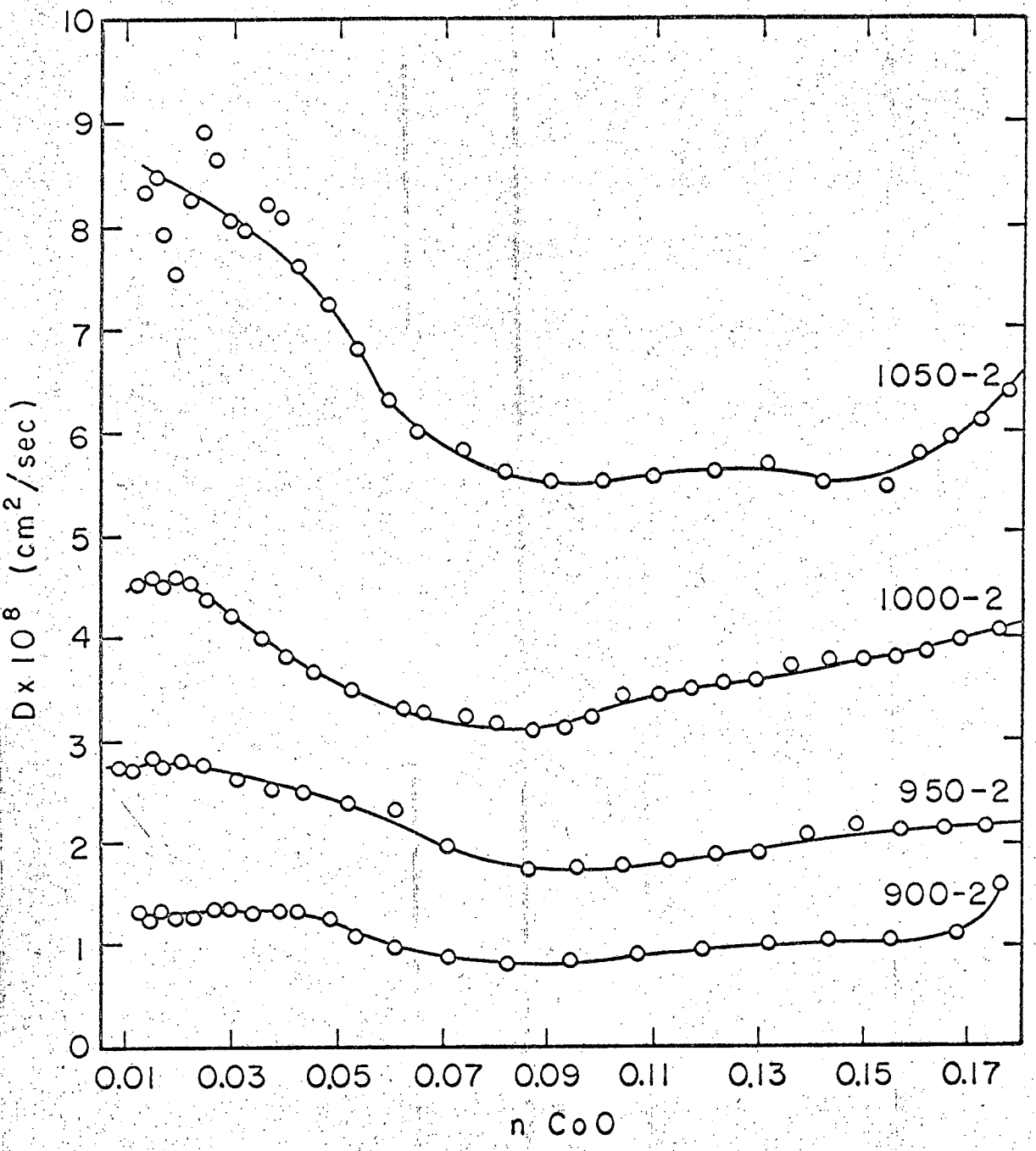

MUB-10893

Fig. 9. Computer determined diffusivities of 2-hour samples.

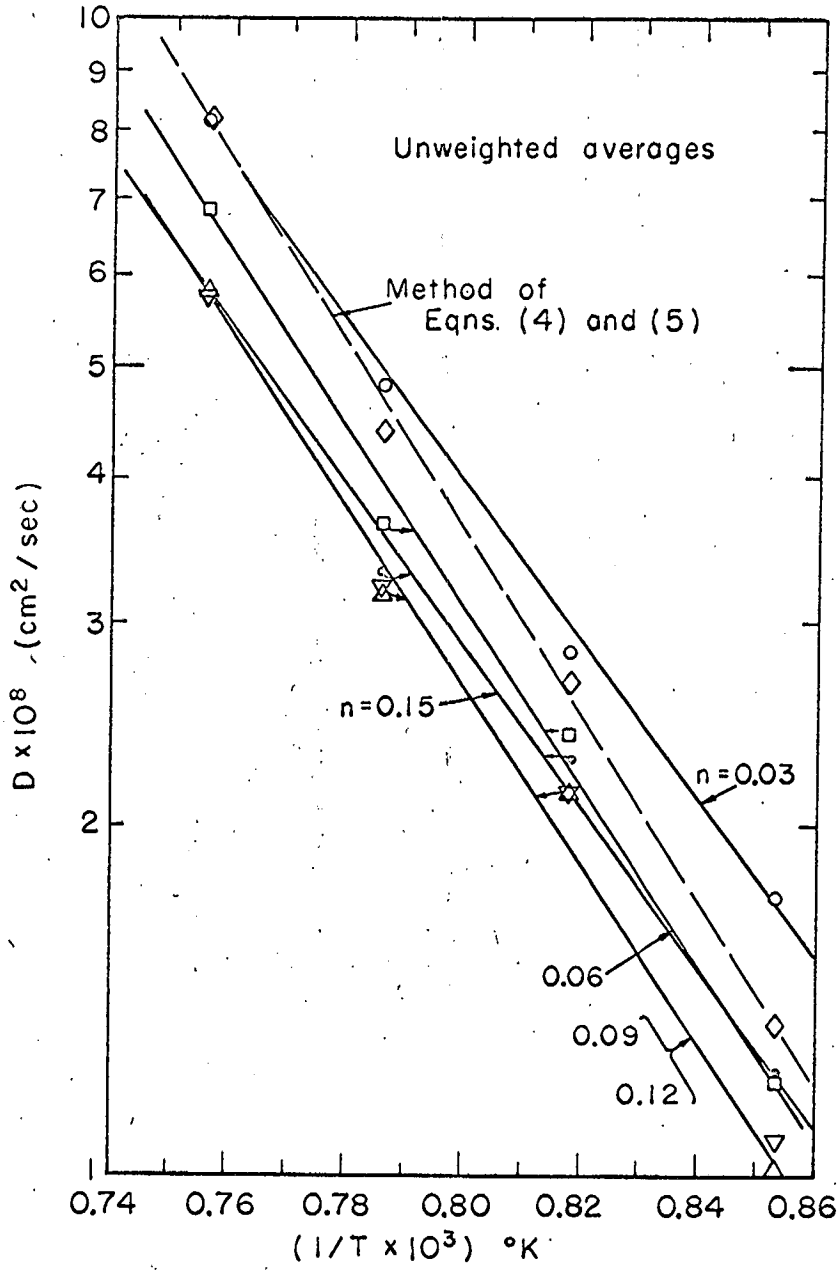

MUB-10888

Fig. 10. Arhennius plots of diffusivities based on Boltzmann-Matano analysis for selected mole fractions of CoO. (Unweighted data)

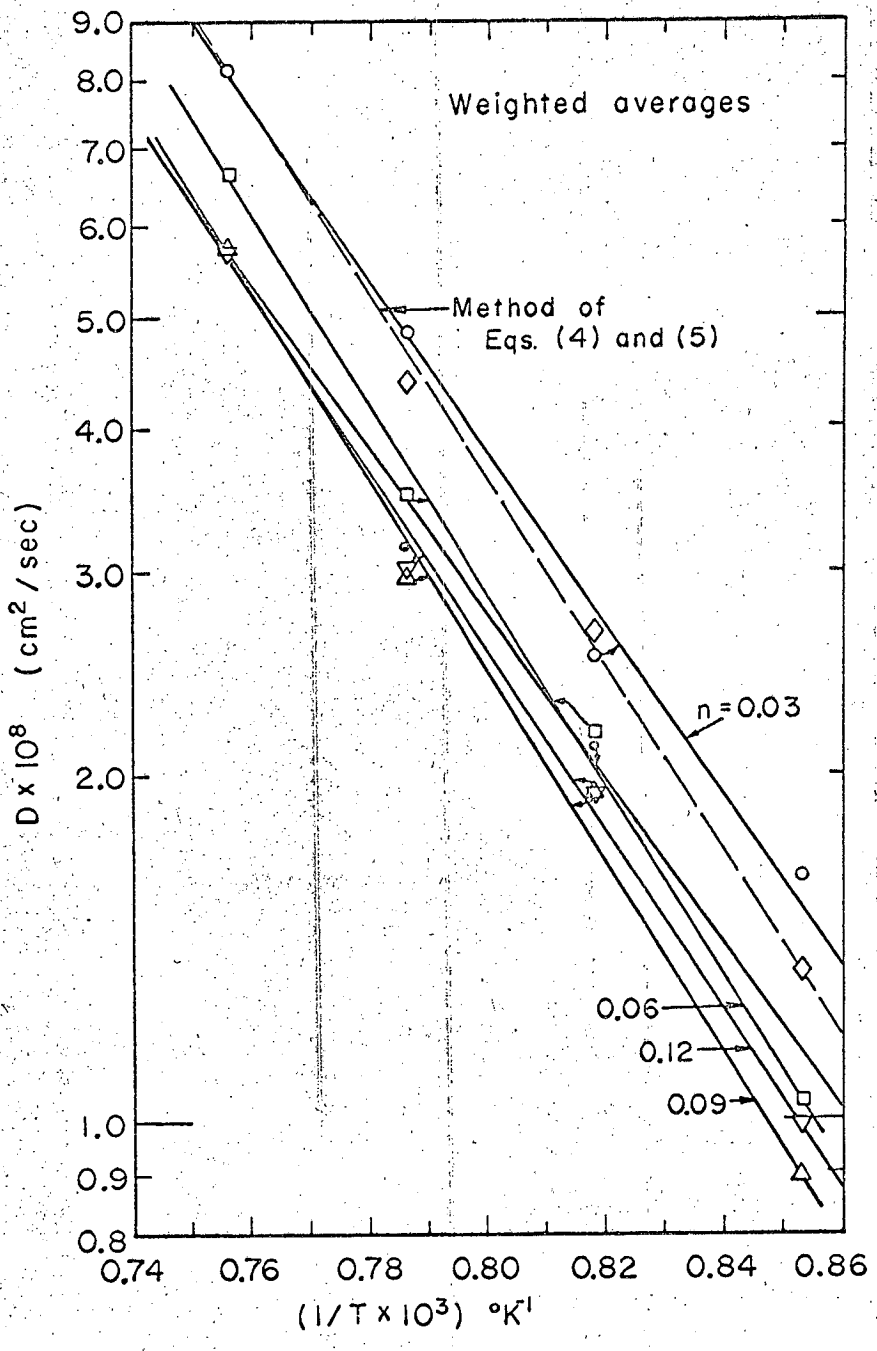

Fig. 11. Arhennius plots of diffusivities based on Boltzmann-Matano analysis for selected mole fractions of CoO. (Data weighted according to diffusion time).

Table IIIa. Temperature variation of diffusivities based on Boltzmann Matano analysis

$D^{*}x10^{8}$ (unweighted data)

1/T	0.853	0.818	0.876	0.756	$D = D_o exp(-\Delta H/RT)$
n_{CoO}					
0.03	1.74	2.83	4.83	8.18	$D=1.48x10^{-2}exp(-31.9/RT)$
0.06	1.20	2.40	3.66	6.85	$D=2.03x10^{-2}exp(-33.3/RT)$
0.09	1.01	2.13	3.19	5.81	$D=3.36x10^{-2}exp(-34.9/RT)$
0.12	1.07	2.13	3.23	5.72	$D=2.31x10^{-2}exp(-33.6/RT)$
0.15	1.22	2.29	3.34	5.84	$D=0.93x10^{-2}exp(-31.3/RT)$

Table IIIb

$D^{**}x10^{8}$ (weighted data)

1/T	0.853	0.818	0.786	0.756	$D = D_o exp(-\Delta H/RT)$
n_{CoO}					
0.03	1.63	2.54	4.85	8.13	$D=2.35x10^{-2}exp(-33.7/RT)$
0.06	1.04	2.16	3.49	6.67	$D=10.47x10^{-2}exp(-37.4/RT)$
0.09	0.89	1.93	2.96	5.71	$D=9.28x10^{-2}exp(-37.1/RT)$
0.12	0.98	1.93	3.00	5.68	$D=4.43x10^{-2}exp(-35.2/RT)$
0.15	1.15	2.13	3.16	5.73	$D=1.27x10^{-2}exp(-32.1/RT)$

$$D^{*} = \frac{D_1+D_2+D_4}{3} \qquad D^{**} = \frac{D_1+2D_2+4D_4}{7}$$

The subscripts 1, 2 and 4 refer to time.

V. DISCUSSION

A. Location of the Matano Interface

In order to apply the Boltzmann approach, the ionic motion must be diffusion-controlled; i.e., the diffusion distance (x) for a given concentration of the diffusing species, must be directly proportional to the square root of time (Eq. (6b)). This was a fundamental assumption made by Boltzmann in obtaining his solution for Fick's second law. The plane defining the origin of x (i.e. $x = 0$) is the Matano interface.

The question of correctly locating this interface for our system now arises. As mentioned on page 16, this author has followed the suggestion of Borom in locating the Matano interface at that point at which a mass balance of dissolved and diffused CoO is obtained. However, a question of the validity of this concept arises when applied to this system of a dissolving oxide layer with no interpenetration of some species diffusing in the opposite direction. This may be illustrated in the following manner:

If one introduces the variable $\varphi = \frac{x}{t^{1/2}}$ into Fick's second law (2), it may be shown that for the initial conditions $t=0$, $c=c_o$ for $x < 0$; $t=0$, $c=0$ for $x > 0$; that the diffusivity D may be expressed as

$$-\frac{1}{2}\int_0^{c'} x\,dc = Dt \left.\frac{dc}{dx}\right|_{c=c}^{c=c'} \qquad \text{where } 0<c'<c$$

If one assumes a diffusion profile after some $t>0$, as in Fig. 8, it may be seen that the condition $\frac{dc}{dx} = 0$, $c=0$. One may directly arrive at the Boltzmann equation as follows:

$$D(c) = -\frac{1}{2t}\frac{dx}{dc}\int_0^{c'} x\,dc \qquad (6)$$

If, now, one assumes the condition $\frac{dc}{dx} = 0$ for $c = c_o$, we have $\int_0^{C_o} x dc = 0$, which defines the plane $x = 0$ by equating the 2 hatched areas. (See Fig. 8.) However, this last boundary condition comes into question when one assumes a diffusion profile as in Fig. 12 and a moving phase boundary, as is the case in our CoO-glass system.

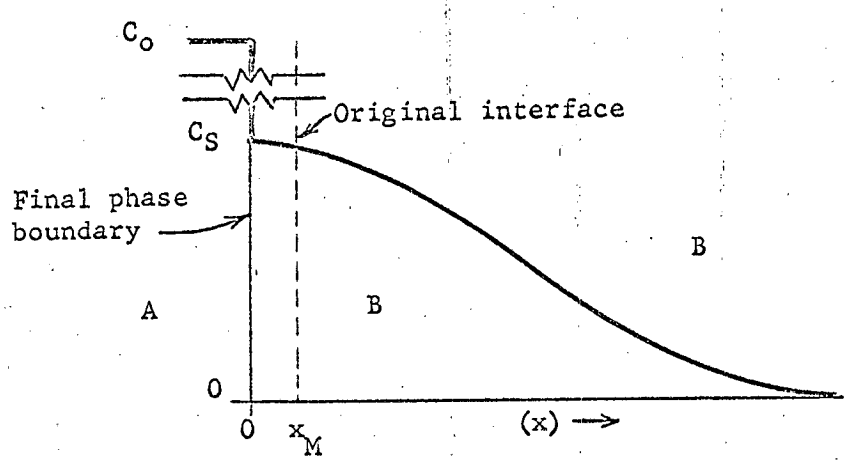

Fig. 12. Schematic diagram of the dissolution and diffusion of species A into B with no interpenetration of B into A.

Consequently, the validity of choosing the Matano interface by analogy to Eq. (10) is questionable. However, the interface chosen by Eq. (10) gives, within experimental error, linear plots of (x) vs. $(t)^{1/2}$, (see Fig. 13), thus allowing one to proceed with a Boltzmann Matano analysis. It should be pointed out that shifting of this interface by small amounts will still give reasonably linear plots, and substantially little change in the calculated diffusivity values.

For example, two hypothetical interfaces were determined, one on the basis that $\rho_{CoO} = 6.45$ and the second based on $\rho_{CoO} = \rho_{glass}$. This then represents the two extremes of possible position of the original interface. Diffusivity calculations based on Boltzmann-Matano

analysis considering both interfaces showed a disagreement of approximately 10%. This is within the spread of values found for different times at any one temperature and is within the tolerances defined by other experimental error.

B. Comparison of the Diffusion of FeO with CoO in NS_2

Since Co and Fe are chemically similar transition metals of period VIII, it would be expected that the divalent oxides CoO and FeO* would show a measure of similarity in their diffusion behavior. Comparison of the results of this work with that of Borom[7] shows indeed that this is so.

In both cases, the dissolution of the oxide appears to be diffusion controlled as evidenced by (1) linear plots of $(M_t)^2$ vs. time (Fig. 6), a constant oxide concentration in the glassy phase at the interface which increases only with temperature and is independent of time (Table II), and (2) a diffusion rate proportional to the square root of time (Fig. 13).

Borom[7] has reported a temperature dependence of FeO in NS_2 (based on calculations of Eq. (4) as $D_{FeO} = 0.692 \times 10^{-2} \exp(-27.8/RT)$, while this study has shown a dependence of $D_{CoO} = 8.05 \times 10^{-2} \exp(-35.4/RT)$.

While no particular significance is attached to the relative D_o values, since they are obtained by a long extrapolation from a short range of data points, it may be noted that there is an increase in activation energy and a decrease in the overall diffusivity for CoO as

---

* (In this thesis the symbol FeO refers to the inherently non-stoichiometric $Fe_{0.947}O$).

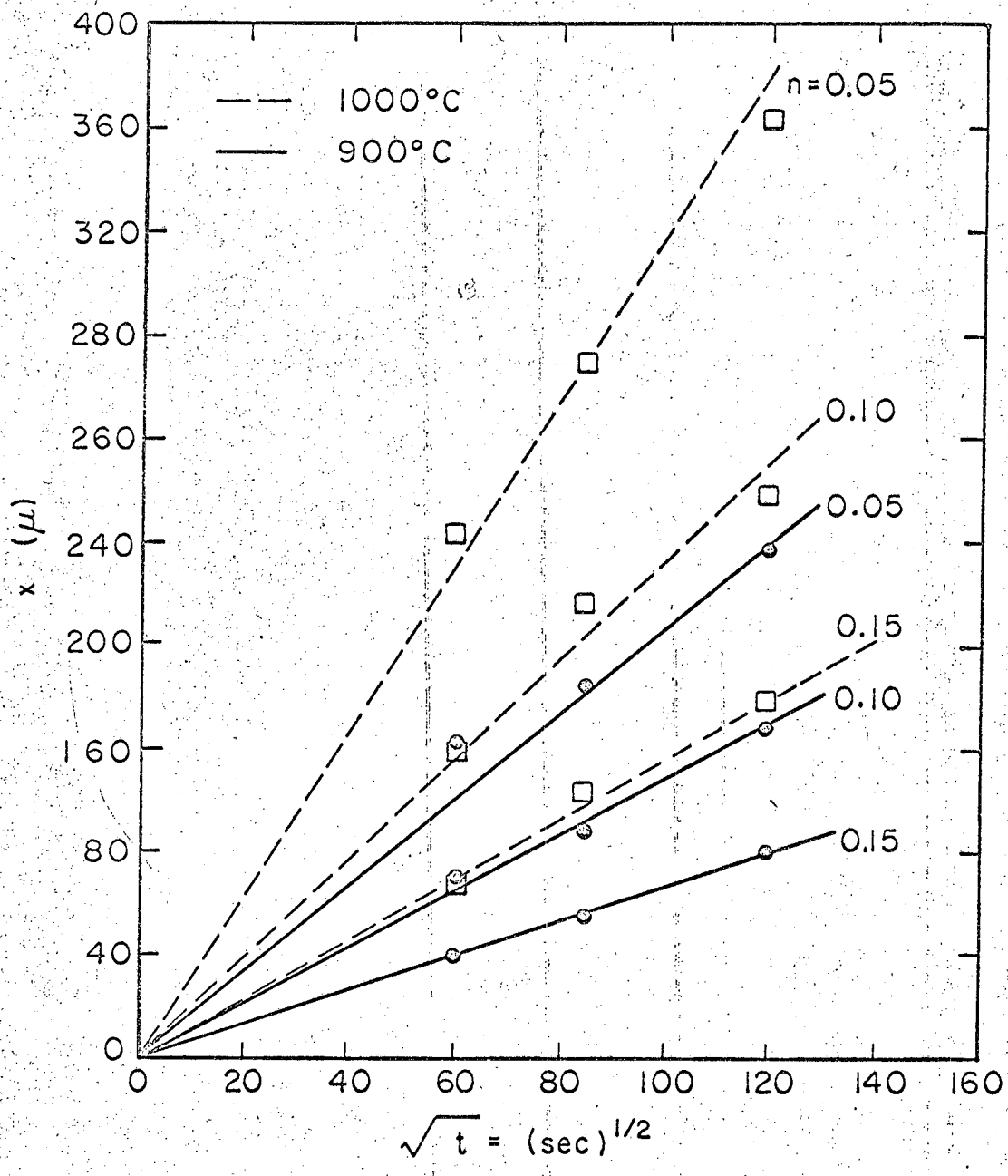

MUB-10890

Fig. 13. 900° C and 1000° C plots of diffusion distance (x) vs. the square root of time for 3 concentrations of Co^{2+} (n = weight fraction of Co^{2+}).

compared with FeO. This is thought to be due to a difference in the atomic polarizabilities of Co^{2+} and Fe^{2+}. A similar phenomenon was found by Wuensch and Vasilos[9] by diffusing Fe^{2+}, Co^{2+} and Ni^{2+} into MgO; and also by Blank[10] in his studies of Fe^{2+} and Ni^{2+} diffusion in MgO. Both investigators found the activation energy to increase in the order Fe^{2+} - Co^{2+} - Ni^{2+}, in spite of a respective decrease in the ionic radius. According to Wuensch and Vasilos (referring to a work by Dienes[11]), there are three major contributions to the activation energy for a lattice jump. These are differences in (1) coulombic attractive energy, (2) overlap repulsive energy, and (3) polarization energy. The latter contribution tends to lower the barrier to diffusion, and includes both polarization of the structure about the particular defect involved in the jump, and polarization of the jumping ion. In an attempt to justify the increase in activation energy of Co^{2+} over Fe^{2+} in NS_2, one may note the following. Due to the similarity in ionic radii (Table IV), it is felt that the coulombic and overlap repulsive energies would be similar for both Co^{2+} and Fe^{2+} ions, or at least have a minor effect on an activation energy difference. Since the matrix for diffusion in both cases is NS_2 glass, it is felt that the polarization of the network would be similar for both Co^{2+} and Fe^{2+}. Finally, we consider the polarizability (α) of the Fe^{2+} and Co^{2+} ions, and here a significant difference is seen. If we consider that the activation energy varies in some way directly with the radius (r) and inversely with the polarizability, we may then correlate the observed activation energy with some undefined quantity which is a function of (r/α). A comparison may be seen in Table IV. Trusting this to be a

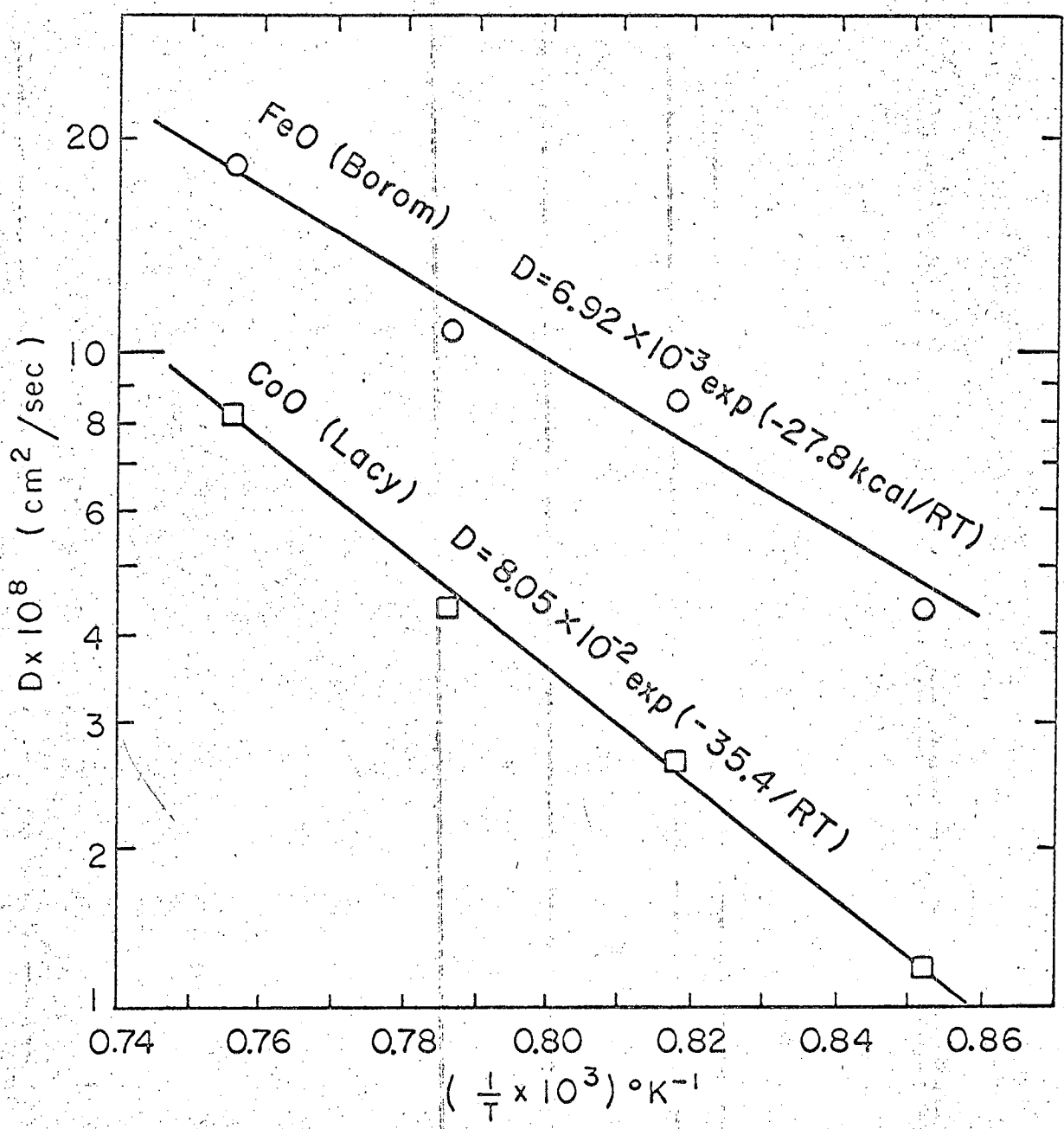

MUB-10892

Fig. 14. Comparative Arhennius plots of the apparent diffusivities of FeO and CoO in NS_2

valid assumption, the activation energy of Ni^{2+} diffusion in NS_2 is roughly predicted.

Since in our case, the D_o values for Fe^{2+} and Co^{2+} diffusion in NS_2 are (within experimental error) nearly the same, the diffusivity of these ions is directly related to the activation energy, thus accounting for the lower diffusivity of Co^{2+} than Fe^{2+} in the glass.

Table IV

Ion	Ni^{2+}	Co^{2+}	Fe^{2+}
Ionic Radius (A)	0.69	0.72	0.75
Ionic Polarizability (α)-($\mathring{A}^3$)	0.246	0.289	0.456
$\frac{r}{\alpha}$ ($\mathring{A}^{-2}$)	2.80	2.49	1.64
Activation Energy for diffusion in NS_2	~36 kcal**	35.1 kcal*	30.4 kcal*

* From Boltzmann Matano Analysis

** Predicted

C. Determination of the Position of the Original Interface Based on a Mass Balance of all Oxides

As discussed in Section VA (page 28), Eq. (10) was used to establish a mass balance leading to the location of the position of the original interface. Once established by Eq. (10) this should then lead also to a balance of SiO_2 and Na_2O on either side of this plane. Such was not found to be the case if one simply equates areas defined by the SiO_2 and Na_2O profile (see Fig. 5). The latter method tends to

define original interfaces at distances roughly twice as far into the glass from the final phase boundary as a CoO balance does. It is felt that this may be accounted for by two explanations:

1. Microscopic examination of the interface shows that the oxide layer exhibits a degree of porosity which one is unable to measure non-destructively. The bulk density of the oxide is then undoubtedly somewhat less than 6.45 as assumed in these calculations. Insertion of a smaller density value into Eq. (10) would tend to increase the distance of the calculated original interface as based on CoO.

2. When one equates areas within the glass itself, a constant density is assumed. It is evident that the density of the glass varies with changing oxide content. Consequently, to achieve a SiO_2 mass balance over the diffusion range, the variable density factor must be included in any calculation. The result of an increasing density nearer the oxide layer would be to displace the previously calculated original interface (based on a SiO_2 balance) nearer the oxide.

The problem of quantitatively defining these corrections is, however, very difficult, and the present CoO balance appears to be adequate for the purpose of numerical calculations.

D. The Question of the Existence of Other Oxides of Cobalt in the System $xCoO\text{-}yNS_2$

It is well known that in a ferrous oxide-glass system, it is very difficult to exclude ferric ions. When one considers a cobalt-oxide-glass couple, the question of the presence of cobaltic (Co^{3+}) ions also arises, since both metals are chemically similar and have stable oxides of the form M_2O_3 and M_3O_4.

According to "Cobalt Monograph",[12] Co_2O_3 decomposes to CoO at 300° C, and Co_3O_4 to CoO at 900° C. The divalent phase (CoO) is stable at all temperatures at low oxygen pressure. Since all experiments were conducted either in environments of vacuum at temperatures below 900° C or in an inert atmosphere at higher temperatures, it is felt that neglibible further oxidation of the CoO could have taken place.

Furthermore, Weyl[13] has used transition metal ions such as Mn, Fe, Co, Ni, V, etc. as coloring ions and has found that all, with the exception of Co and Ni, exist in different valency states in glass. Cobalt enters the glass as Co^{2+} and is not affected by either oxidizing or reducing conditions. From this it is established that the cobaltous ion is the only form present in the diffusion couple.

E. Comment

A final point brought to light by these studies is that, due to the apparently small concentration dependence of diffusivity, a very good approximation of the diffusivity and activation energy may be obtained without the use of computers, involved programs and great monetary expense. This is evidenced by the nearly identical results of Eqs. (4) and (8), and the Boltzmann-Matano analysis.

VI. CONCLUSIONS

From the results of this study it is concluded that

(1) The dissolution of CoO in sodium disilicate glass is diffusion controlled.

(2) The diffusivity of Co^{2+} in NS_2 shows a very small dependence in concentration at temperatures below 950° C with a very slight increase in this dependence at higher temperatures.

(3) The diffusivity of Co^{2+} is lower and activation energy higher than that of Fe^{2+} over the temperature interval studied, and that this may be attributed to a significant decrease in the ionic polarizability of Co^{2+} over Fe^{2+}.

(4) There is a definite uncertainty in the location of the Matano interface and also the original interface prior to diffusion, but this uncertainty introduces only small error into the calculations based on Boltzmann-Matano analysis.

(5) Reasonably reliable diffusion data may be obtained in this system using simple mathematical analysis, without the aid of computers.

VII. ACKNOWLEDGMENT

The author wishes to extend his sincere appreciation to Professor Joseph A. Pask and Dr. Marcus P. Borom for their helpful criticism, guidance, and encouragement. Further thanks are also extended to Professor John Dorn, Dr. Bernard Evans, and all my fellow colleagues for their most valuable discussions of the problems at hand.

This work was done under the auspices of the United States Atomic Energy Commission.

VIII. REFERENCES

1. J. Crank, Mathematics of Diffusion (Clarendon Press, Oxford, 1956)
2. A. Fick, "Uber Diffusion", Poggendorff's Annalen 94 59 (1855)
3. P. G. Shewmon, Diffusion in Solids, (McGraw-Hill, N.Y., 1963)
4. W. Jost, Diffusion in Solids, Liquids & Gases (Academic Press, N.Y. 1931)
5. L. Boltzmann, Ann. Phys., Leipzig 53 p. 959 (1894)
6. C. Matano, Japan Journ. Phys. 8 109 (1933)
7. M. P. Borom, "Kinetics of the Dissolution and Diffusion of the Oxides of Iron in Sodium Disilicate Glass", Lawrence Radiation Laboratory Report UCRL-16232, August 1965
8. A. Z. Trapsl - LRL, Berkeley. Laboratory routine program for calculating diffusivities
9. B. J. Wuensch & T. Vasilos, Jour. Chem. Phys. 36 (11) 2917-22 (1962)
10. S. L. Blank - Lawrence Radiation Laboratory Annual Report, UCRL-11889 p. 149 (1964) Berkeley, California
11. G. J. Dienes, J. Chem. Phys. 16 620 (1948)
12. "Cobalt Monograph" ed. by Centre D'Information Du Cobalt, pp. 129-31 (1960)
13. W. A. Weyl, "Coloured Glasses, Part II--The Colour of Glasses Produced by Various Colouring Ions", Jour. Glass Tech. 28 158 (1944)

This report was prepared as an account of Government sponsored work. Neither the United States, nor the Commission, nor any person acting on behalf of the Commission:

A. Makes any warranty or representation, expressed or implied, with respect to the accuracy, completeness, or usefulness of the information contained in this report, or that the use of any information, apparatus, method, or process disclosed in this report may not infringe privately owned rights; or

B. Assumes any liabilities with respect to the use of, or for damages resulting from the use of any information, apparatus, method, or process disclosed in this report.

As used in the above, "person acting on behalf of the Commission" includes any employee or contractor of the Commission, or employee of such contractor, to the extent that such employee or contractor of the Commission, or employee of such contractor prepares, disseminates, or provides access to, any information pursuant to his employment or contract with the Commission, or his employment with such contractor.